Development 128, 3635-3647 (2001)
Printed in Great Britain © The Company of Biologists Limited 2001
DEV3373

Regulation of cell polarity, radial intercalation and epiboly in *Xenopus*: novel roles for integrin and fibronectin

Mungo Marsden and Douglas W. DeSimone*

Department of Cell Biology, University of Virginia Health System, School of Medicine, PO Box 800732, Charlottesville, VA, 22908-0732, USA
*Author for correspondence (e-mail: dwd3m@virginia.edu)

Accepted 18 June 2001

SUMMARY

Fibronectin (FN) is reported to be important for early morphogenetic movements in a variety of vertebrate embryos, but the cellular basis for this requirement is unclear. We have used confocal and digital time-lapse microscopy to analyze cell behaviors in *Xenopus* gastrulae injected with monoclonal antibodies directed against the central cell-binding domain of fibronectin. Among the defects observed is a disruption of fibronectin matrix assembly, resulting in a failure of radial intercalation movements, which are required for blastocoel roof thinning and epiboly. We identified two phases of FN-dependent cellular rearrangements in the blastocoel roof. The first involves maintenance of early roof thinning in the animal cap, and the second is required for the initiation of radial intercalation movements in the marginal zone. A novel explant system was used to establish that radial intercalation in the blastocoel roof requires integrin-dependent contact of deep cells with fibronectin. Deep cell adhesion to fibronectin is sufficient to initiate intercalation behavior in cell layers some distance from the substrate. Expression of a dominant-negative β1 integrin construct in embryos results in localized depletion of the fibronectin matrix and thickening of the blastocoel roof. Lack of fibronectin fibrils in vivo is correlated with blastocoel roof thickening and a loss of deep cell polarity. The integrin-dependent binding of deep cells to fibronectin is sufficient to drive membrane localization of Dishevelled-GFP, suggesting that a convergence of integrin and Wnt signaling pathways acts to regulate radial intercalation in *Xenopus* embryos.

Key words: Integrin, Fibronectin, Gastrulation, Epiboly, Cell polarity, *Xenopus*

INTRODUCTION

During embryogenesis, the morphogenetic processes that direct the basic architecture of the gastrula are driven through localized cell rearrangements (Keller and Winklbauer, 1992; Keller, 1980b). While many of the cellular movements involved have been described in some detail, we know little of the molecules that guide them. Early in development fibronectin (FN) is assembled into extracellular matrices (ECMs) that are essential for normal morphogenesis (DeSimone, 1994; Hynes, 1990). FN-null mice are embryonic lethal and have defects in mesodermal derivatives (George et al., 1993). Similarly, FN matrix is required for the post-involution migration of mesoderm in chick embryos (Harrisson et al., 1993). Amphibian embryos assemble a fibrillar FN matrix along the inner aspect of the blastocoel roof (BCR) during gastrulation (Boucaut and Darribere, 1983a; Boucaut and Darribere, 1983b; Collazo et al., 1994; Lee et al., 1984; Nakatsuji and Johnson, 1983; Nakatsuji et al., 1985). In salamander embryos, injection of specific function-blocking antibodies or other reagents that selectively interfere with FN binding to cells inhibits gastrulation by disrupting mesoderm involution and migration (Boucaut and Darribere, 1983a; Boucaut and Darribere, 1983b; Darribere et al., 1990; Darribere et al., 1988). Because mesodermal explants and dissociated cells from amphibian embryos also migrate on FN substrates in vitro (Darribere et al., 1988; Nakatsuji, 1986; Riou et al., 1990), it was concluded that the FN-dependent migration of mesoderm along the BCR was a key process driving gastrulation. However, the range of embryonic defects attributed to FN loss-of-function defects at gastrulation in these and other embryos cannot easily be accounted for solely by global disruptions in mesoderm migration. Therefore, while it is clear that FN has multiple functions in vertebrate gastrulation, a specific role outside of mesoderm migration remains to be defined.

In contrast to salamanders and other vertebrate embryos, the FN matrix of the BCR in *Xenopus laevis* has been suggested by some investigators to play a minor, if any, role in gastrulation. While FN has been shown to support *Xenopus* mesoderm migration in vitro (Winklbauer, 1990), the disruption of integrin/FN interactions in vivo does not block gastrulation, as defined by eventual blastopore closure and mesoderm involution (Howard et al., 1992; Ramos and DeSimone, 1996; Ramos et al., 1996; Winklbauer, 1989; Winklbauer and Keller, 1996; Winklbauer and Stoltz, 1995).

Keller and Jansa have further shown that involution and dorsal mesoderm extension occur even in the absence of a BCR (Keller and Jansa, 1992), suggesting that the primary mechanism regulating dorsal mesoderm movement in *Xenopus* is convergent extension. However, others have reported that inhibition of integrin/FN interactions in *Xenopus* results in delayed blastopore closure, axial defects and ectodermal thickening (Johnson et al., 1993; Ramos and DeSimone, 1996; Ramos et al., 1996). This indicates that FN may play more subtle but important roles in multiple morphogenetic processes at gastrulation.

Recent evidence obtained from *Xenopus* (Djiane et al., 2000; Medina et al., 2000; Medina and Steinbeisser, 2000; Tada and Smith, 2000) and zebrafish (Heisenberg et al., 2000) suggests that cell-cell adhesion is regulated through the Wnt/Fz signaling pathway at gastrulation. Convergent extension is inhibited in *Xenopus* explants overexpressing the Fz7 receptor, but this defect can be rescued by co-expressing a dominant-negative construct of CDC42, a member of the Rho family of small GTPases (Djiane et al., 2000). Gastrulation defects resulting from disruptions in the Wnt signaling pathway may arise from a loss of planar cell polarity (PCP) in marginal zone cells (Djiane et al., 2000; Wallingford et al., 2000). The establishment of PCP in *Xenopus* is presumed to involve interactions of members of the wingless/Wnt family with frizzled receptors (Djiane et al., 2000; Tada and Smith, 2000). Thus, it appears that cell adhesion and cell polarity pathways converge in these embryos and interact to regulate cell rearrangements at gastrulation. Integrin/ligand interactions have also been tied to the establishment of cell polarity, and the differentiation of MDCK cells and keratinocytes (Ojakian and Schwimmer, 1994; Watt et al., 1993). It has been proposed that integrin/ECM engagement provides initial spatial cues that help set up subsequent epithelial cell polarity (Yeaman et al., 1999). Interestingly, in mouse (George et al., 1993), chick (Harrisson et al., 1993) and amphibians (Johnson et al., 1993), disruption of integrin/FN interactions results in ectodermal epithelial defects that could be interpreted as stemming from a loss of cell polarity.

We have re-examined the role that FN plays in *Xenopus* gastrulation using monoclonal antibodies (mAbs) that inhibit FN/integrin interactions and matrix assembly in vivo. We show that FN is required for the cellular rearrangements that drive epiboly in the marginal zone at gastrulation. Integrin-based interactions with FN are necessary for the establishment of cell polarity in the deep layers of the dorsal marginal zone (DMZ) and BCR. These polarized cells either participate actively in intercalative behaviors in the DMZ or are required to maintain epithelial integrity in the BCR.

MATERIALS AND METHODS

Embryos and antibodies and surface labeling

Xenopus laevis albino and wild-type adults were purchased from Xenopus 1 (Ann Arbor, MI). Embryos were obtained and cultured using standard methods. The 1F7, 4B12 and 4H2 mAbs were prepared and injected as described previously (Ramos and DeSimone, 1996). Microinjected embryos were fixed in 3.7% formaldehyde in phosphate-buffered saline (PBS) for 2 hours at room temperature and vitelline envelopes removed manually. Fixed embryos were stored in methanol at –20°C until used for immunostaining. Embryos stained for tubulin were prepared as described previously (Gard, 1993). For confocal microscopy, dejellied albino embryos were injected with 10 nl of 40 mg/ml Ruby Red lysinated dextran (10,000 M_r; Molecular Probes, Eugene OR) 20 minutes postfertilization.

Dextran-labeled embryos were surface biotinylated at stage 9 using 1 mg/ml sulfo-NHS biotin (Pierce) in 0.1×MBS (modified Barth's saline) for 5 minutes. Embryos were washed extensively in 0.1×MBS with 100 mM Tris-HCl (pH 7.4) to quench exogenous biotin. Embryos were injected with antibody as described above and fixed at stage 17. Biotin labeling was detected with strepavidin-HRP using Fluorescein Tyramide as a substrate (Davidson and Keller, 1999). Embryos were bisected and processed for confocal microscopy as described below.

Confocal microscopy

Embryos stored in methanol were rehydrated in PBS/0.05% Tween-20 (PBST), bisected with a scalpel and processed for immunostaining. Embryo halves were blocked for 2 hours in PBST/DMSO (PBS, 0.1% Triton X-100, 1% DMSO, 5% calf serum) and incubated in primary antibody diluted in PBST/DMSO (rabbit anti-FN polyclonal 1:1000, mouse anti-tubulin 1:1000, mouse or rabbit anti-hemagglutinin (HA) 1:500) overnight mat 4°C. Embryos were washed and incubated overnight in appropriate secondary antibodies in PBST/DMSO. Embryos were washed extensively in PBST, dehydrated in methanol, cleared in BBA (benzyl alcohol/benzyl benzoate) and mounted for confocal microscopy as described (Davidson and Keller, 1999). Images were collected on a Zeiss CSLM 400.

Embryos were stained with anti-tubulin antibody, as described above, in order to determine spindle orientation. Sagittal and oblique confocal sections of bisected embryos were used to determine spindle orientation in deep and superficial layers of the BCR. For a spindle to be counted out of the BCR epithelial plane, the axis of the spindle had to be 45° or more away from the plane of the epithelium.

Digital image capture and timelapse

Antibody-injected embryos were mounted in clay wells in 0.1× MBS and digital images captured with Isee software (Innovision, Raleigh NC) using a Hamamatsu Orca camera mounted on a Zeiss Axiophot microscope. A motorized stage (Ludl) allowed for serial capture of images at 1 minute intervals from nine sibling embryos in each experiment. Morphometric measurements were made using the Isee software.

HAβ1 constructs

The integrin HAβ1 construct was produced by subcloning the Xenopus β1 cytoplasmic tail (starting at amino acid 752) onto the extracellular and transmembrane domains of viral hemagluttinin (Doms, 1986). The entire construct was subcloned into the pSP64T vector (D. G. Ransom, PhD thesis, University of Virginia). This construct will be described in detail elsewhere (B. J. Dzamba et al., unpublished). RNA transcripts were produced from the pSP64T vector by standard methods and injected into the animal poles of embryos at the four-cell stage. Expression of the HA constructs was detected with a mouse monoclonal anti-HA antibody (site A; a gift from Judith White).

Deep cell layer explants

Fertilized eggs were injected with dextran as described above. At stage 10, DMZs were cut from labeled embryos and the deep cell layers lining the blastocoel were teased free from the superficial and underlying 'intermediate' layers. The labeled deep cell layers were typically 2-3 cell layers thick. A labeled deep cell fragment was then placed on either FN (20ug/ml) or BSA-coated coverslips. The DMZ from an unlabeled embryo was excised and, after removal of the deep cell layers lining the blastocoel, the region consisting of the superficial and intermediate deep cells (2-3 layers) was used to overlay the labeled fragment on the substrate. Explants were kept flat with a small fragment of coverslip anchored with silicone grease. Explants were

cultured in Danilchik's solution for up to 3 hours and cell intercalation recorded by digital image capture. Explants were fixed in 3.7% formaldehyde in MEMFA (0.1 M Mops, pH 7.4, 2 mM EGTA, 1 mM $MgSO_4$), dehydrated, cleared in BBA, mounted and examined by confocal microscopy as described above.

Dsh-GFP localization assays

Differential recruitment of the Dishevelled (Dsh) protein to the cell membrane was assayed using DMZ explants. 50 pg of synthetic XDsh-GFP RNA (a gift from S. Sokol) was injected into fertilized eggs prior to first cleavage. This amount of XDsh-GFP had no discernable effect on normal development. At stage 10, dorsal marginal zones were cut from embryos and trimmed to remove involuting marginal zone tissue, placed on bovine serum albumin (BSA)-coated coverslips, or on coverslips that had been previously coated with various adhesive substrates (0.23 μM plasma FN, GST fusion proteins, or 10 μM poly-lysine) and blocked with mAb 4B12 and/or BSA (1% solution). Preparation of the 9.11-GST and Hep II-GST fusion proteins is described elsewhere (Ramos and DeSimone, 1996). XDsh-GFP localization was monitored by confocal microscopy over a 2 hour period.

RESULTS

Anti-FN antibodies block FN fibril assembly

In an effort to elucidate a definitive role for fibronectin in gastrulation, we have made use of antibodies that specifically block integrin interactions with the RGD (mAb 4B12) or synergy sites (mAb 1F7) located within the central cell binding domain (CCBD) of *Xenopus* FN (Ramos and DeSimone, 1996; Ramos et al., 1996). Blastocoelar injection of these mAbs before the onset of gastrulation completely blocked assembly of FN fibrils (Fig. 1C,D). The inability to assemble a fibrillar matrix was not due to antibody crosslinking of FN, as injection of another mAb (4H2) directed against the CCBD of FN did not inhibit fibril assembly (Fig. 1B). Because mAb 4H2 had no measurable effect upon FN assembly or embryonic development (Ramos et al., 1996), it was used as a control in all subsequent experiments. Data for uninjected or sham injected control embryos (Fig. 1A) were indistinguishable from embryos injected with mAb 4H2, and are not shown in subsequent figures. Similarly, no differences were noted between mAb 1F7- and mAb 4B12-injected embryos at these stages and, therefore, data for both these function-blocking mAbs are not included in all figures.

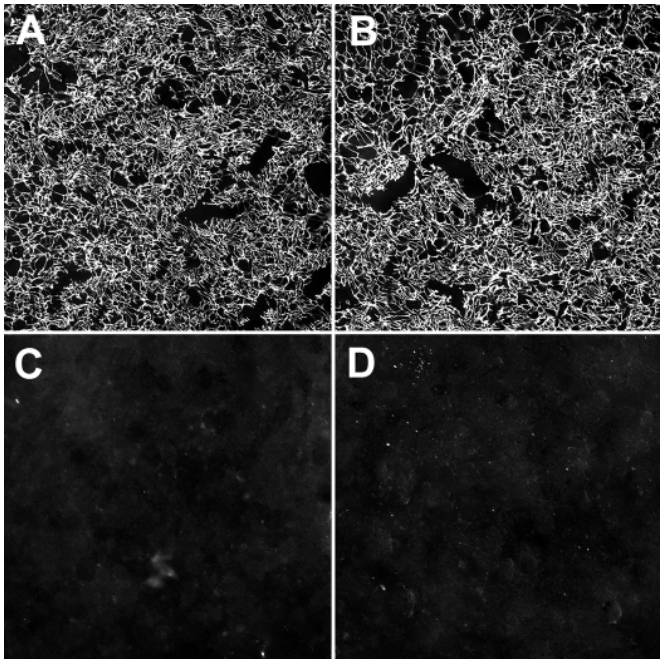

Fig. 1. Anti-FN mAbs inhibit matrix assembly in vivo. Embryos were injected with a mouse mAb and FN detected with an anti-FN rabbit polyclonal. (A) BCR of stage 11.5 sham-injected embryo showing normal FN fibril formation. (B) BCR of sibling embryo injected with the non-blocking anti-FN mAb 4H2. (C) Injection of mAb 1F7 directed against the synergy site of FN inhibits BCR matrix assembly at stage 11.5. (D) mAb 4B12 directed against the RGD-containing central cell-binding domain of FN.

FN is required for normal gastrulation

Embryos that lacked fibrillar FN matrix underwent gastrulation, as measured by the ability to close the blastopore, and go on to form tadpoles (Fig. 2). However, these embryos revealed a progressive increase in developmental defects during gastrulation and beyond (Fig. 2D-F,H). Dorsal lip formation and early involution appeared normal until stage 10.5 (compare Fig. 2A,B with Fig. 2D,E). By stage 11, it was evident that embryos injected with function blocking mAbs exhibited a delay in blastopore closure (Fig. 2E), as described previously (Ramos and DeSimone, 1996), and eventually developed into tadpoles that were arched anteriorly and truncated along the anterior/posterior axis (Fig. 2F). Tadpoles retained the remnants of the blastocoel that had been displaced ventrally (Fig. 2F). Most of these embryos developed into tadpoles with head defects, including small eyes, and also typically lacked blood, blood vessels, hearts and gut structures (Fig. 2H). Some of these late phenotypes were probably secondary consequences of defects arising at gastrulation and we are presently investigating the morphogenetic movements of the mesendoderm in these embryos (L. A. Davidson, B. G. Hoffstrum, M. M. and D. W. D., unpublished).

The cellular rearrangements of mAb-injected embryos were examined by confocal microscopy (Fig. 3). Initially, at stage 10+ both control and experimental embryos appeared very similar; blastopores formed and deep mesoderm movements initiated (Fig. 3A,E). By stage 11, it was clear that control embryos assembled FN along the BCR (arrowhead Fig. 3B), while embryos injected with function-blocking mAb had not (Fig. 3F). The latter embryos lacked an archenteron at stage 11 and bottle cells remained at the surface of the embryo (compare Fig. 3C with Fig. 3G). This did not represent simply a delay in gastrulation because, despite a lack of bottle cell ingression, the deep endoderm and mesoderm still extended along the blastocoel walls (compare Fig. 3B with Fig. 3F). In control embryos the extension of mesoderm and endoderm was greater along the dorsal side of the embryo (Fig. 3B). However, extension appeared equal along both dorsal and ventral surfaces of the BCR in embryos injected with FN function-blocking mAb (Fig. 3F). At stage 12, it was evident that the gross morphology of embryos treated with function blocking antibodies was severely disrupted (Fig. 3H). Cell-cell contacts in the ventral endoderm became dissociated in the

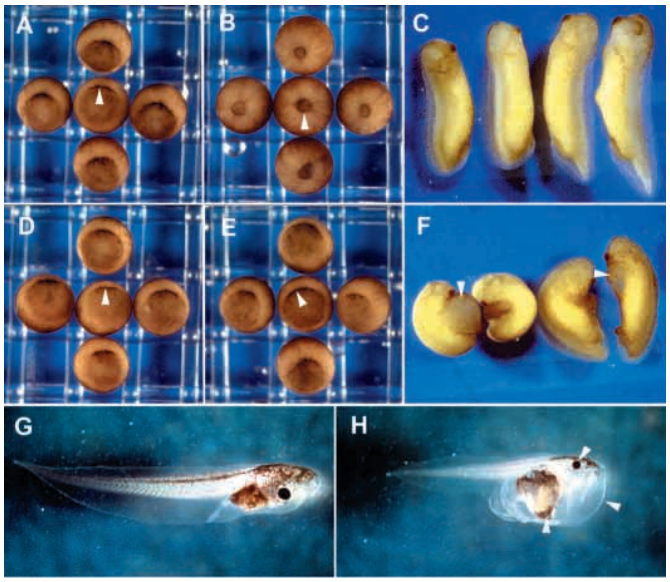

Fig. 2. Intra-blastocoelar injection of anti-FN mAbs disrupts gastrulation. (A-C,G) Embryos injected at stage 9.5 with mAb 4H2 show normal development at stage 10.5, as indicated by dorsal lip formation (A, arrowhead). (B) At stage 11.5 the blastopore is almost closed (arrowhead) and embryos go onto develop into tadpoles (C,G). mAb 1F7-injected embryos (D-F,H) develop a normal blastopore at stage 10.5 (D, arrowhead). (E) By stage 11.5, there is a significant delay in blastopore closure and little movement of the blastopore lip is apparent (arrowhead). (F) mAb 1F7-injected embryos are truncated along the AP axis and bent ventrally. The blastocoel is retained and displaced ventrally (arrowhead). (H) Blastulae injected with mAb 1F7 develop into tadpoles that have small eyes, display head edema, and lack gut (arrowheads), heart, blood vessels and blood.

area of the yolk plug. The endoderm and mesoderm continued to extend towards the animal pole but the blastocoel was displaced centrally and a normal archenteron failed to form. Although the mesoderm moved toward the animal pole, it did not adhere to the BCR (Fig. 3H) and the mesendodermal mantle did not close. In control embryos, the axial mesoderm and neural plate had begun to differentiate by this stage. These embryos displayed a normal expanded archenteron and the blastocoel was reduced (Fig. 3D).

FN matrix is required for epiboly

Aside from defects in involution and the subsequent mesendoderm movements described above, we noted that the BCRs of embryos injected with FN function-blocking mAbs progressively thickened during gastrulation (e.g. Fig. 3F,H). In normal gastrulae, the BCR thins through radial intercalation of deep layers and spreads through epiboly to encompass the embryo. Epiboly occurs in two distinct phases beginning in the animal cap before the initiation of gastrulation and spreading

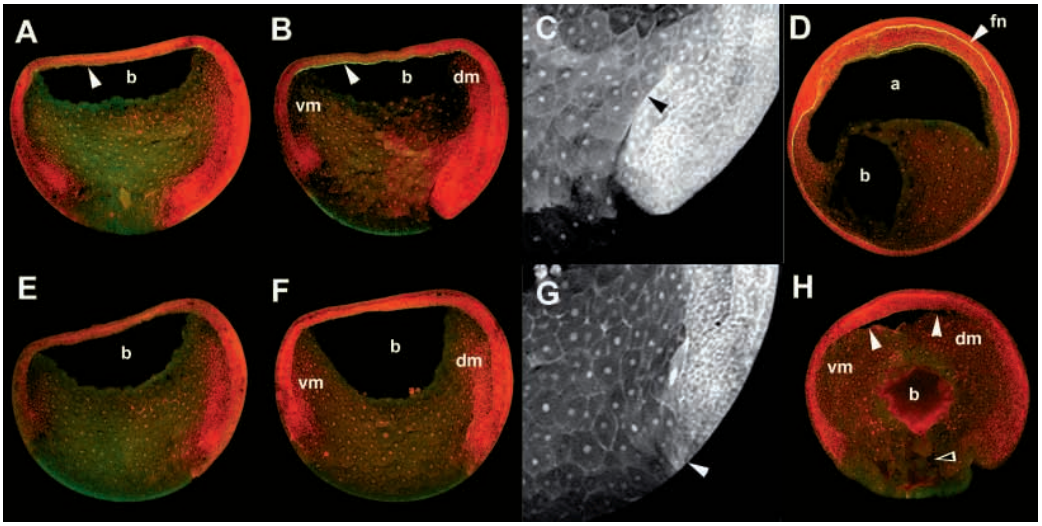

Fig. 3. Sagittal sections of gastrula stage embryos. In all panels embryos are arranged with the dorsal lip towards the right. MAb 4H2- (A-D) and mAb 1F7-injected (E-H) embryos were optically sectioned by confocal microscopy. Dextran (red) is used for contrast enhancement as described in the methods. FN is detected with a rabbit polyclonal Ab (green). The intracellular green fluorescence observed in endoderm and mesoderm cells results from autofluorescence and does not represent FN localization. Stage 10.5 mAb 4H2-(A) and mAb 1F7-injected (E) embryos look similar. FN accumulates along the BCR in mAb 4H2-injected embryos (A, arrowhead) and does not accumulate in embryos injected with mAb 1F7 (E). (B) Stage 11 embryos injected with mAb 4H2: displacement of involuted mesoderm is greater along the dorsal side of the embryo (dm). (F) Stage 11 mAb 1F7-injected embryos show an equal displacement of dorsal (dm) and ventral (vm) mesoderm. (C) Archenteron formation in mAb 4H2-injected embryo is evident by stage 11 (arrowhead). (G) Bottle cells (arrowhead) remain on the surface of stage 11 mAb 1F7-injected embryos and no archenteron is evident. (D) By stage 12, mAb 4H2-injected embryos exhibit a closed blastopore and an inflated archenteron (a). The blastocoel (b) is almost eliminated, and mesoderm has begun to differentiate. A pronounced FN matrix (fn) is evident (D, arrowhead). Gastrula injected with mAb 1F7 shows misplaced mesoderm that is not adherent to the BCR (H, arrows). The BCR has thickened and the marginal zones remain thick. No archenteron is present and a centralized remnant of the blastocoel remains. The blastopore remains open and tissue in the yolk plug appears dissociated (H, open arrow). a, archenteron; b, blastocoel; bcr, blastocoel roof; dm, dorsal mesoderm; fn, fibronectin matrix; vm, ventral mesoderm. QuickTime movies of blastopore closure of control and mAb injected embryos may be viewed on the DeSimone laboratory website (http://faculty.virginia.edu/desimonelab).

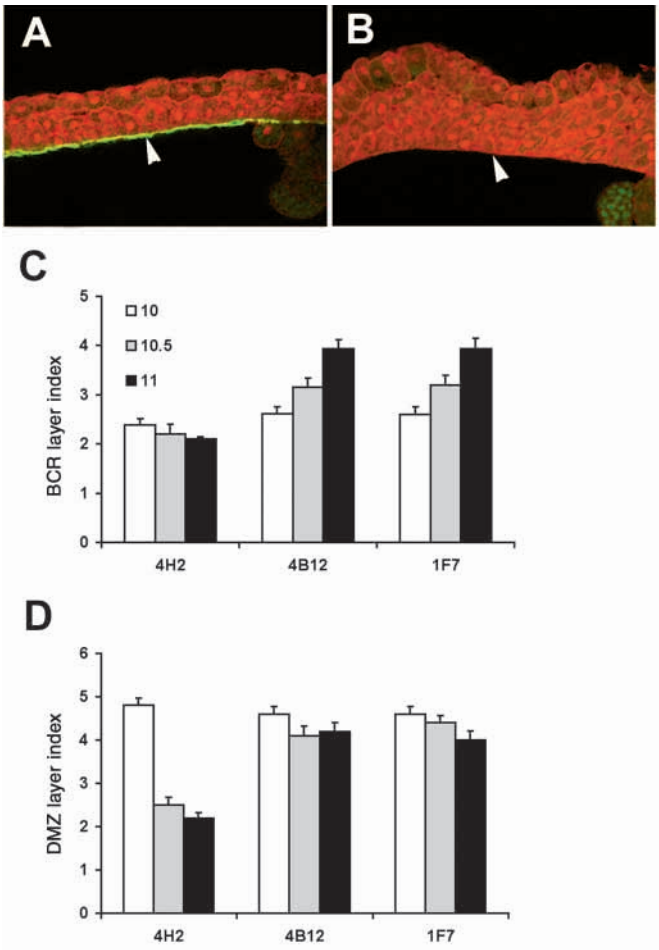

Fig. 4. FN is required for BCR and DMZ thinning. Blastocoelar injection of mAbs was performed at stage 9.5. (A) Confocal section of the BCR of mAb 4H2-injected dextran-labeled embryo at stage 11. The FN matrix lining the blastocoel is shown (arrowhead). There is only a single layer of deep cells (layer index=2). (B) mAb 1F7-injected dextran labeled embryos at stage 11. No FN matrix is evident (arrowhead) and the BCR has multiple layers of deep cells. (C) BCR layer index of mAb-injected embryos. MAb 4H2-injected embryos (controls) show a decrease in BCR layer index from 2.3 at stage 10 to 2 by stage 11. In mAb 4B12-injected embryos, the BCR shows an increase in BCR layer index from 2.4 at stage 10 to almost 3.9 by stage 11. Similarly, in mAb 1F7-injected embryos the layer index increases from 2.4 at stage 10 to 3.9 at stage 11. (D) DMZ layer index does not decrease in blocking mAb-injected embryos. In mAb 4H2-injected embryos (controls) the DMZ layer index decreases from 4.9 at stage 10 to 2.2 at stage 11. In mAb 4B12-injected embryos, the layer index at stage 10 is 4.8 and this decreases to 4.6 by stage 11. In mAb 1F7-injected embryos the layer index at stage 10 is 4.8 and this decreases to 4.2 by stage 11. The minimum number of cells spanning the BCR in the radial direction was counted (layer index) at stages 10 (white bars), 10.5 (gray bars) and 11 (black bars).

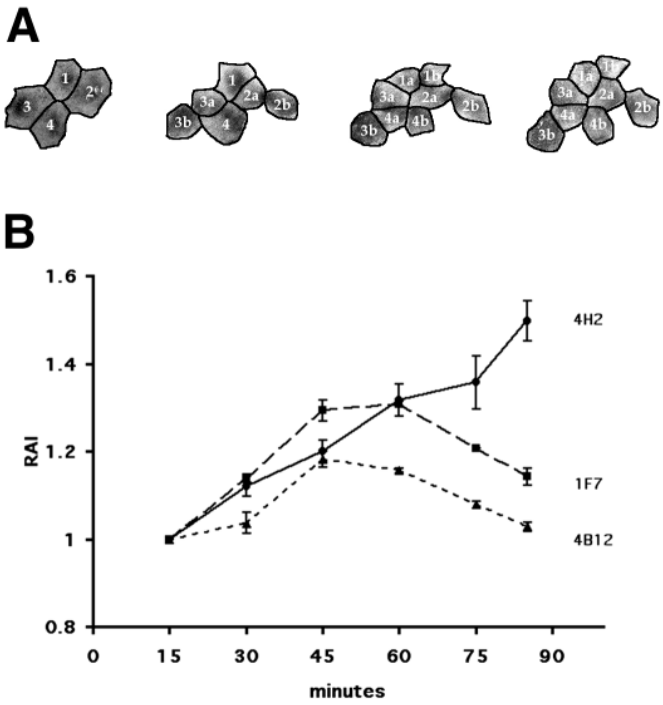

Fig. 5. The relative area index (RAI) was estimated from digital images captured from DMZ during early and mid-gastrulation. This measurement compares the relative area occupied by cells and all clonal derivatives during gastrulation (Keller, 1978). (A) Samples of DMZ RAI tracings for a 4H2-injected embryo are shown. Numbers indicate original cells in group, while letters indicate daughter cells. (B) The RAI in mAb 4H2 embryos increases throughout gastrulation (unbroken line). In mAb 1F7- (dashed line) and mAb 4B12- (dotted line) injected embryos there is an initial increase in the RAI until stage 10.5, followed by a decrease in later gastrulation.

to the marginal zones as gastrulation proceeds (Keller, 1978). The early thinning of the animal cap occurs before FN fibril assembly begins and injection of function-blocking mAbs before stage 9 had little or no effect on this early phase of epiboly (data not shown). In embryos injected with the control mAb, a FN matrix was assembled (Fig. 4A, arrowhead) and the roof thinned from a layer index of 3 to a layer index of 2, as expected (Fig. 4C). In embryos injected with blocking mAbs, a matrix was not assembled (Fig. 4B, arrowhead) and the BCR in the animal cap regions of these embryos progressively thickened from a layer index of two to a layer index of 4, owing to an increase in the number of cells occupying the deep layers of the BCR (Fig. 4C). This suggests that FN is not required for the initial thinning of the roof, but is required to maintain these cellular rearrangements later in gastrulation.

In the dorsal marginal zone the situation is more complex. The blastocoel walls have a layer index of 5 at stage 10+ (Fig. 4D). In control embryos at stage 12, a fibrillar FN matrix was assembled across the BCR and the marginal zones thinned to a layer index of 2 through radial intercalation movements (Fig. 4D). When FN fibrillogenesis was blocked with mAb 1F7 or mAb 4B12 the marginal zones did not thin by stage 12 and the layer index remained at 4-5 (Fig. 4D). The arrangement of the deep cell layers of the marginal zone roof revealed that these cells did not undergo radial intercalation, indicating that FN matrix is required in this area for normal morphogenesis. This suggests that in the marginal zone, FN matrix plays an active role in the thinning of the BCR during gastrulation.

Epiboly is correlated with the spreading of the superficial layer of the BCR. The relative area index (RAI; Keller, 1978) is a measure of the area occupied by the clonal derivatives of a population of superficial cells (Fig. 5A). In embryos injected

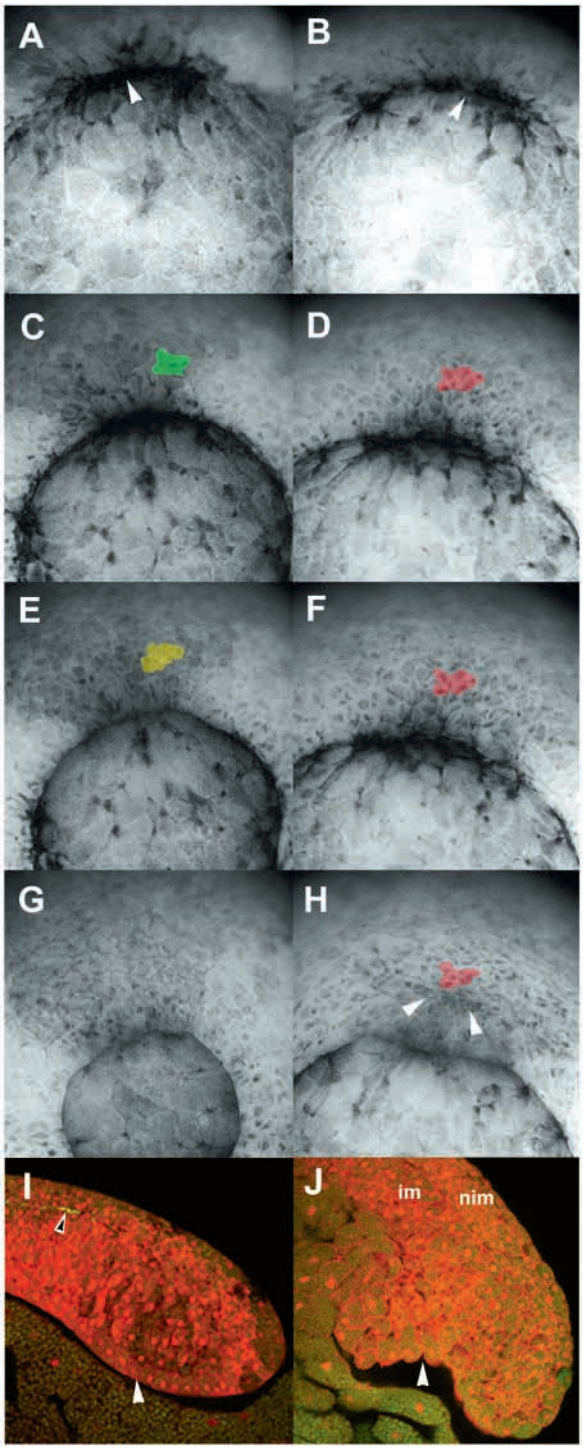

Fig. 6. Timelapse microscopy of dorsal lip movement. (A,C,E,G,I) mAb 4H2-injected control embryos. The blastopore closes normally and there is a progressive involution of superficial DMZ cells over the blastopore lip. (A) Bottle cell formation is normal (arrowhead), and cells marked in green in the DMZ at stage 10.5 (C) before involution over the lip. (E) At stage 11 cells marked in green have passed over the lip to contribute to the lining of the archenteron. A second population of cells marked in yellow also passes through the blastopore as it closes (G). (I) Cross sections through the blastopore lip of stage 12 mAb 4H2-injected embryos reveal involuted superficial cells lining the archenteron (white arrowhead). A FN matrix (black arrowhead) separates the BCR deep cells from the involuted mesoderm. (B,D,F,H,J) Embryos injected with mAb 1F7. In these embryos there is no migration of DMZ cells over the lip of the blastopore during the same time period. (B) Blastopore lip formation is normal (arrowhead). (D,F,H) Cells marked in red remain essentially in the same position in DMZ, and the blastopore remains open through stage 12. Before blastopore closure, the DMZ buckles (arrows H,J). In mAb 1F7-injected embryos, there is no FN matrix evident and the involuted mesoderm (im), as well as the non-involuted tissue (nim) in the DMZ, appears to be disorganized. No archenteron has developed and the short invagination (arrowhead) is the result of DMZ buckling. QuickTime movies of the embryos used to obtain still images for Fig. 6A-H may be viewed on the DeSimone laboratory website (http://faculty.virginia.edu/desimonelab).

with the control mAb 4H2, there was a steady increase in the DMZ RAI during gastrulation (Fig. 5B). In embryos injected with either function-blocking mAb, the DMZ RAI showed an initial increase, before decreasing later in gastrulation (Fig. 5B). There was no loss of daughter cells in any of the clonal lineages examined, so the decrease in RAI reflects a decrease in surface area of superficial cells in the mAb 4B12- and mAb 1F7-injected embryos. The lack of superficial layer spreading during mid-gastrulation correlated temporally and spatially with lack of radial intercalation in the marginal zone (Fig. 4). The decrease in RAI seen in these embryos probably reflects a certain amount of compression observed in the DMZ before buckling at later stages (see below).

A temporal analysis of the cell movements in the superficial layer of the marginal zone in mAb-injected embryos provided further evidence that epiboly was inhibited in the absence of FN matrix. By following superficial cells proximal to the dorsal lip, it was clear that populations of cells in control mAb 4H2-injected embryos began to involute starting at stage 10+ and continued until late in gastrulation (Fig. 6A,C,E,G). These cells went on to form the lining of the archenteron (Fig. 6I, white arrowhead). In contrast, by following populations of cells in the DMZ of embryos injected with blocking mAbs, it was evident that superficial cells that normally involute to form the lining of the archenteron remained on the surface of the embryo throughout gastrulation (Fig. 6B,D,F,H). The area proximal to the dorsal lip in these embryos eventually buckled (Fig. 6H arrowheads) to form a shallow invagination seen in confocal sagittal section (arrow Fig. 6J). In control embryos, the involuted mesendoderm appeared organized and the radial orientation of these cells indicates they were undergoing radial intercalation (Fig. 6I). By contrast, the involuted mesoderm of function blocking-mAb 1F7-injected embryos was disorganized and the cells took on no obvious orientation (Fig. 6J).

To examine further the involution of surface cells to form the lining of the archenteron, embryos were cell-surface biotinylated at stage 9, injected with antibodies at stage 9.5, and fixed at stage 17 (Fig. 7). In control embryos, the archenteron formed normally (Fig. 7A) and was outlined after staining for biotin (arrow Fig. 7C), indicating that superficial cells had involuted to line the archenteron. In embryos injected with blocking mAb the involuted mesendoderm (im) did not appear to be organized (Fig. 7B). There was no archenteron and the blastocoel (b) was retained (Fig. 7B). In these embryos, biotin staining is limited to dorsal and ventral bottle cells

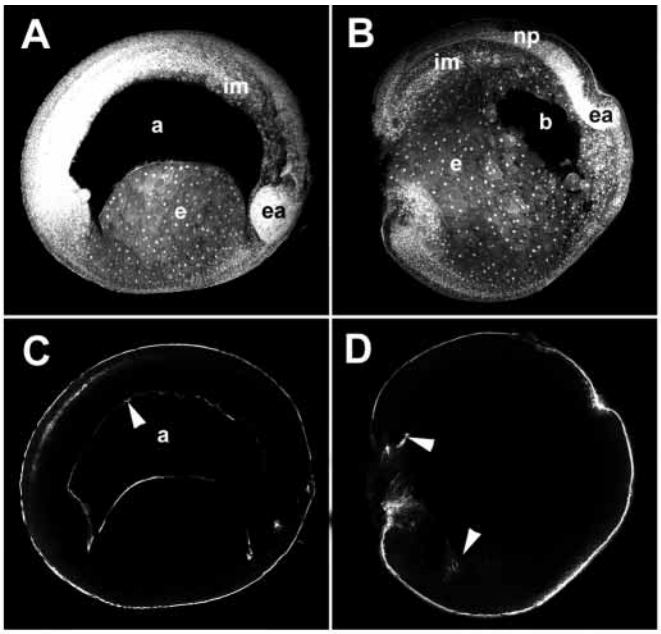

Fig. 7. FN is required for archenteron formation. Embryos are arranged with anterior to the right. (A,B) Confocal sections of stage 17 embryos collected on the red channel, showing dextran labeling in all cells in the embryo. (C,D) The same sections as in A and B collected on the green channel to reveal biotin-labeled cells detected with fluorescein tyramide. (A) Embryos injected at stage 9.5 with mAb 4H2 go on to develop normal neurula with an enlarged archenteron (a). Involuted mesoderm (im) is differentiating and endoderm (e) is contained ventrally. The eye anlage (ea) has begun to differentiate. (C) Biotin labeling of cell surface at stage 9 reveals that the archenteron lining is derived from cells that were previously at the surface of the embryo (arrowhead). (B) Embryos injected with mAb 1F7 have a short AP axis, the archenteron fails to form and the blastocoel (b) is retained. The neural plate has formed (np) and the eye anlage (ea) is evident. The endoderm (e) is not ventrally contained and the involuted mesoderm (im) is disorganized. Biotin labeling reveals that few surface-labeled cells involute inside the embryo (D; arrowheads).

(arrow Fig. 7D), indicating a limited degree of superficial cell involution.

FN regulates cell behaviors in the blastocoel roof

The inability of antibody-treated embryos to undergo epiboly in the absence of FN suggests that the underlying morphogenetic behaviors are supported by the FN matrix. We devised a novel explant culture system to test whether FN could promote radial intercalation behavior in the BCR (Fig. 8A, see Materials and Methods for full description). In the 'reconstituted' BCR explant, labeled deep cell layers of the BCR (i.e. cell layers normally in closest apposition with FN fibrils in vivo) were placed on a FN substrate and overlain with a non-labeled BCR that lacked deep cell layers. Under these conditions, the labeled patch of cells was 'broken up' by the intercalation of more 'superficial' unlabeled cells that invaded the labeled patch (Fig. 8C,E,G). Moreover, when viewed in cross section, it was apparent that this behavior was transmitted across cell layers some distance from the FN matrix, with many labeled and unlabeled cells apparent at multiple levels (Fig. 8I). We found no evidence that cells initially in contact

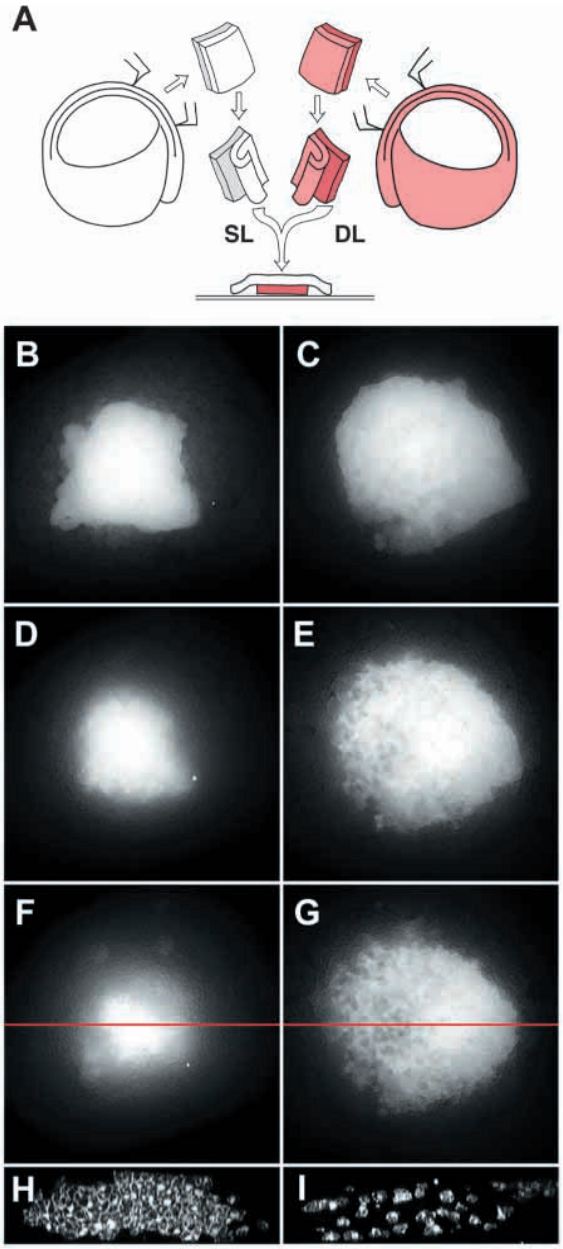

Fig. 8. Intercalative behaviors in the BCR. We developed an in vitro deep layer explant to examine intercalative behaviors in a reconstituted BCR. The assay took place over 120 minutes. (A) DMZ zone tissue was cut from dextran labeled (red) embryos and layers of deep cells lining the blastocoel (DL) were shaved from the explant and placed on substrate (FN or BSA) coated coverslip. A similar DMZ fragment was cut from unlabeled embryo and the superficial layer and a few layers of deep cells (SL) were used to overlay the labeled tissue. Intercalative behavior was monitored by image capture of the deep layer of the explant. On BSA (B,D,F,H), the labeled patch incorporated into the BCR. Vertical confocal sectioning (red line in F) showed that the tissue remained coherent (H). When explants are plated on FN, the labeled patch was broken up by intercalating cells (C,E,G,I). Vertical sections of the explant (red line in G) showed that unlabeled cells intercalated between labeled cells distant from the substrate (I).

with the FN substrate lost adhesion to the substrate during the timecourse of the assay. When a similar explant was cultured

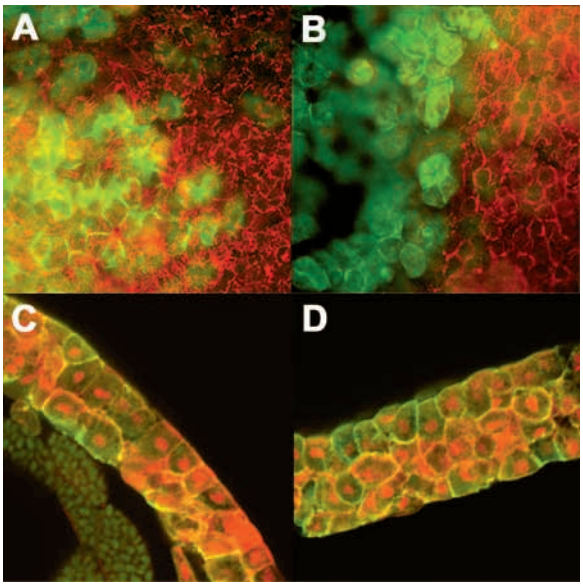

Fig. 9. Intercalative behaviors require β1-containing integrins. Two-cell embryos were injected in one blastomere with either 1 ng HA RNA (control) or the same amount of dominant-negative HAβ1 chimera RNA. (A,C) Expression of HA has no effect upon FN matrix assembly (A; HA in green, FN fibrils in red, overlap in yellow) or on BCR thickness (C; HA shown in green, dextran for contrast is red). (B,D) Expression of the HAβ1 construct results in reduced FN fibril assembly (B; HA in green, FN fibrils in red; faint green cells under fibrils are in the superficial layer), and causes an increase in roof thickness (D; HAβ1 shown in green, dextran for contrast in red).

on BSA, the labeled patch of cells was incorporated into the non-labeled BCR (Fig. 8B,D,F). Over a period of 120 minutes the labeled cells on BSA did not dissociate but were integrated into the roof as a contiguous patch (Fig. 8H). These results suggest that FN can provide a signal that allows cells to undergo intercalative-type movements in the plane perpendicular to the BCR matrix, and that these signals can act at a distance from the FN substrate.

Intercalation behaviors require β1 containing integrins

The mAbs used in this study block the interaction of cells with the CCBD of FN, which contains the RGD and synergy sites. Because inhibition of synergy site recognition was effective in disrupting FN fibril assembly, it is likely that integrin α5β1 is responsible for assembling the BCR matrix, as previously demonstrated in cultured cells (Sechler et al., 1997). In *Xenopus*, the α5β1 receptor is expressed by all cells of the BCR (Gawantka et al., 1994). In order to determine if integrins are involved in the FN matrix-dependent thinning of the BCR, we used a dominant negative construct composed of the β1 integrin cytoplasmic domain fused to the transmembrane and extracellular domains of viral hemaglutinin (HA). HAβ1 expression can be correlated with both the loss FN-matrix assembly (Fig. 9A,B) and an increase in BCR thickness (Fig. 9C,D). Fig. 9B demonstrates that areas of the BCR that expressed the HAβ1 construct did not assemble a FN matrix. A control construct consisting of HA alone had no effect on fibril assembly (Fig. 9A). Areas of the BCR that expressed the

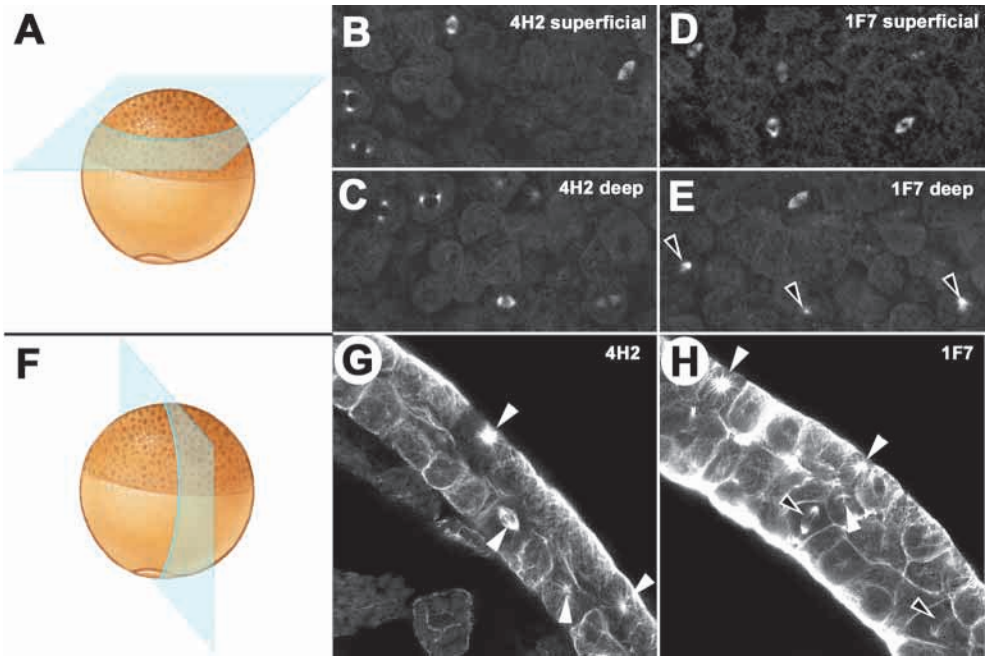

Fig. 10. FN is required for mitotic spindle orientation. (A) Cartoon of stage 11.5 embryo, showing approximate plane of confocal sections (oblique) through the BCR epithelium to visualize en face views of mitotic spindles in both superficial (B,D) and deep (C,E) cell layers. In control (4H2 injected) embryos, the spindles in the superficial (B) and deep (C) cell layers are oriented parallel to the BCR inner surface. In embryos injected with mAb 1F7, spindle orientation in the superficial layer is within the plane of the BCR epithelium (D), while in the deep layers mitotic spindle orientation is randomized (E; arrowheads indicate spindles that are out of the horizontal plane of the epithelium. (F) Cartoon of sagittal confocal section through gastrula embryo. The BCR is two layers thick and the mitotic spindles are in the plane of the epithelium in both cell layers of control embryos injected with mAb 4H2 (G; white arrowheads). In embryos injected with mAb 1F7, spindle orientation in the deep layers is randomized (H; black arrowheads indicate spindles that are not in the plane of the epithelium, while white arrowheads indicate spindles that orient in the plane of the epithelium). Note that arrowheads with asterisks (G,H) indicate spindles in the horizontal plane of the epithelium but the view is down the long axis of the spindle. Fluorescence along the inner BCR surface in B is artifactual and due to precipitation of primary mAb that occasionally occurs during whole embryo fixation.

HA control construct thinned to two layers as expected (Fig. 9C), while patches of the BCR expressing the HAβ1 construct were three to four cell layers thick (Fig. 9D).

FN matrix directs mitotic spindle orientation

Because the FN matrix was correlated with radial intercalation movements and cell rearrangements at some distance from the substrate (Fig. 8), we investigated the possible effects of FN matrix on cell polarity in vivo. In embryos that lacked a FN matrix, the layer index of the BCR deep cells in the marginal zone did not change, while in the animal pole the layer index increased. This suggested that these deep cells had lost their normal orientation with respect to neighboring cells. To further investigate this possibility, we examined the orientation of cleavage planes in the BCR at gastrulation. Normally BCR cell division occurs in the horizontal plane of the epithelium, with the long axis of individual mitotic spindles orientated anywhere within a 360° circle that lies parallel to this plane. One or both spindle poles can be seen in confocal cross section or, alternatively, when looking 'down the barrel' of a spindle, no poles are observed (e.g. Fig. 10F,G). In each case, however, the long axis of the spindle is oriented parallel to the BCR surface; this is clearly demonstrated by en face confocal sections of the BCR (Fig. 10A) where both poles of each spindle are observed in superficial (Fig. 10B) and deep (Fig. 10C) cell layers but, like compass needles, they can normally 'point' in any direction. In control embryos with normal FN matrix, 96% of the mitotic spindles (24 out of 25 mitotic indices counted in five experiments) were orientated parallel to the BCR surface (Fig. 10B,C,G, white arrowheads). In embryos that lacked FN matrix, 56% of the mitotic spindles (14 out of 25 mitotic indices counted in five experiments) were not parallel to the horizontal plane of the BCR (Fig. 10E,H, black arrowheads). This randomization of spindle orientation was observed only in the deep layers of the BCR, while spindle orientation in the single layer of superficial cells remained unchanged (Fig. 10D,H, white arrowheads). This indicates that the observed effects on cell polarity are limited to the deep cells of the BCR and not the outermost single layer of superficial cells.

FN matrix triggers XDsh localization

The randomization of spindle orientation in the absence of a FN matrix suggests that the deep cells of the BCR require FN to maintain polarity. Recent evidence has indicated that cells of the DMZ acquire polarity during gastrulation and that this allows for convergent extension of the mesoderm (Djiane et al., 2000; Tada and Smith, 2000; Wallingford et al., 2000). The localization of Dishevelled (Dsh) has been used as an indication of planar cell polarity (PCP) in *Xenopus* (Axelrod et al., 1998; Rothbacher et al., 2000; Wallingford et al., 2000) and we have used a similar assay to determine whether FN is capable of mediating a similar response in the BCR. We looked at the localization of XDsh-GFP in the non-involuting dorsal marginal zone (NIDMZ) at stage 10, before the assembly of a FN matrix. When explanted DMZs were placed on a BSA substrate, XDsh-GFP localized to the cytoplasm of individual cells and had a granular appearance (Fig. 11A). When the DMZ was placed on a FN substrate the XDsh-GFP moved to the cell membrane (Fig. 11B). The membrane relocalization of XDsh-GFP required FN as poly-L-lysine does not support XDsh-GFP movement (Fig. 11C). Furthermore, adhesion to the CCBD of FN is required because non-integrin-dependent adhesion to the HepII domain does not result in significant XDsh-GFP relocalization (Fig. 11D).

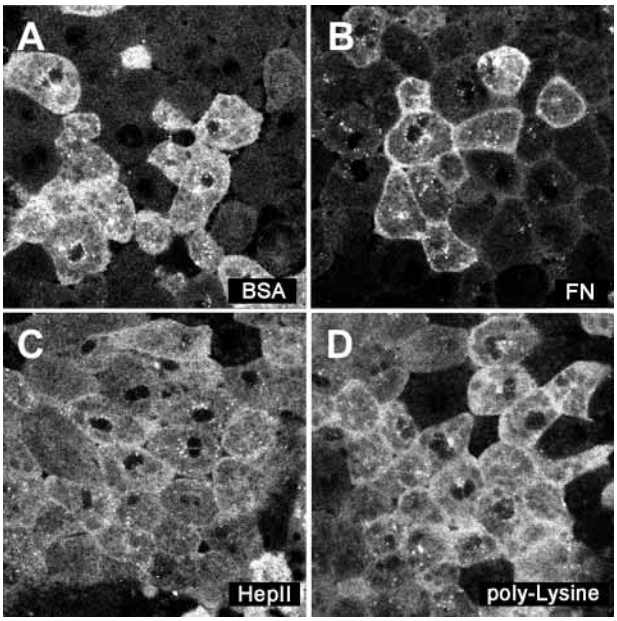

Fig. 11. FN is permissive for XDsh relocalization in the BCR. Embryos were injected with 50 pg of XDsh-GFP RNA. Stage 10 explanted tissue was placed on FN or BSA substrates and examined by confocal microscopy. (A) DMZ tissue placed on BSA shows a granular cytoplasmic localization of XDsh-GFP after 60 minutes. (B) DMZ tissue placed on FN. XDsh-GFP is localized to the cell membrane after 60 minutes. (C) DMZ on the HepII-GST fusion protein. XDsh remains cytoplasmic after 60 minutes. (D) DMZ on poly-L-lysine. XDsh-GFP remains cytoplasmic after 60 minutes.

XDsh-GFP was translocated to the plasma membrane within 1 hour of plating DMZ explants on the fusion protein GST-9.11 (Ramos and DeSimone, 1996), which contains the synergy and RGD-containing CCBD sites of *Xenopus* FN (Fig. 12A-C). The specificity of this response to the CCBD was demonstrated by the failure of XDsh-GFP to localize to the plasma membrane if FN substrates were first incubated with mAb 4B12 before plating the explants (Fig. 12D). This indicates that the XDsh distribution we observe is mediated via integrin binding to FN. That FN adhesion was permissive for XDsh-GFP relocalization was supported by the observation that the animal cap region of the BCR at stage 9 also showed XDsh-GFP relocalization after adhering to GST-9.11 (Fig. 11E). This relocalization was again blocked significantly when the FN substrate was first incubated with mAb 4B12 (Fig. 11F). These results suggest that integrin adhesion to the CCBD of FN is required for XDsh mobilization in BCR cells.

DISCUSSION

FN requirements in gastrulation

We present evidence that the FN matrix lining the BCR in *Xenopus* embryos is essential for deep cell intercalation behaviors at gastrulation. FN matrix assembly is initiated along

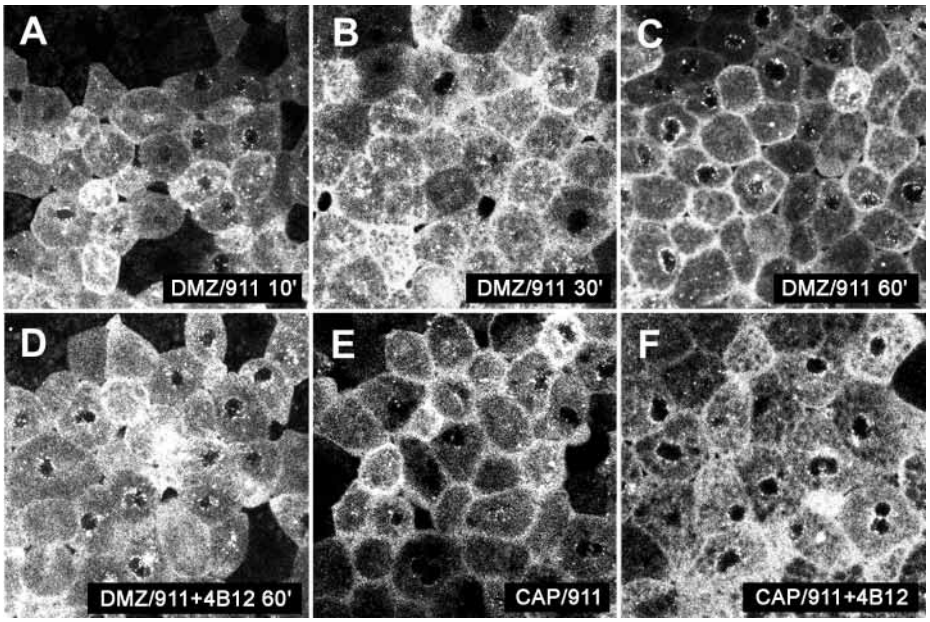

Fig. 12. Timecourse of XDsh-GFP membrane localization. DMZ explants were cultured on GST-9.11 fusion protein substrates. (A) 10 minutes post-plating, XDsh-GFP remained cytoplasmic. (B) After 30 minutes, XDsh-GFP was beginning to accumulate at the cell membrane. (C) 60 minutes after being placed on the substrate, XDsh-GFP was localized to the cell membrane. (D) DMZ explants cultured on GST-9.11 fusion protein pre-incubated with mAb 4B12. XDsh-GFP remained cytoplasmic. (E) When animal caps (CAP) were cultured on GST-9.11 fusion protein, XDsh-GFP was localized to the cell membrane after 60 minutes. (F) The translocation of XDsh-GFP to the cell membrane was blocked after pre-incubation of the substrate with mAb 4B12.

the marginal zone before stage 10.5 in *Xenopus* and progresses towards the animal pole of the BCR as gastrulation proceeds. Injection of either mAb 4B12 or mAb 1F7 (Ramos and DeSimone, 1996; Ramos et al., 1996) effectively eliminates fibril assembly during gastrulation and causes a shortened axis, as well as other deficiencies in tadpoles. Interestingly, in embryos that lack an assembled FN matrix, the temporal acquisition of embryonic defects is coincident with the normal temporal pattern of FN matrix assembly. In stage 11 embryos without a FN matrix, the non-involuting DMZ tissue appears disorganized, and the ventral progression of the dorsal lip is inhibited. Surprisingly, involution of deep mesoderm around the blastopore lip is not inhibited and the dorsal extension of post-involution mesoderm suggests that morphogenetic movements are partially operative in the absence of a FN matrix. The delayed symmetrical closure of the blastopore, lack of superficial ectoderm involution and the shortened axis suggests that convergent extension movements (Keller et al., 1992a) may be disrupted. These observations are in good agreement with those obtained in *Pleurodeles* using FN fragments, site-specific antibodies (Darribere et al., 1992) and recombinant FNs (Darribere and Schwarzbauer, 2000).

Disrupting FN matrix assembly delays, but does not block, blastopore closure. The cellular rearrangements that drive blastopore closure are not clear. However embryos that lack a BCR roof can still close the blastopore (Keller and Jansa, 1992). This indicates that the majority of the morphogenetic processes behind blastopore closure are independent of the BCR, and supports our observation that closure is independent of FN matrix. Embryos treated with LiCl display a similar phenotype at gastrulation, with delayed blastopore closure, symmetrical dorsal and ventral mesoderm involution and a failure of epiboly (Cooke and Smith, 1988; Kao and Elinson, 1988; Klein and Moody, 1989; Regen and Steinhardt, 1988). Despite these defects, blastopore closure still occurs in these embryos. These data suggest that blastopore closure proceeds through a cascade of steps and that more than one mechanism is involved. Disrupting FN matrix assembly probably inhibits cell rearrangements early in the process, but mechanisms acting later can compensate to close the blastopore.

It is likely that that the short axis observed in mAb-injected embryos reflects a lack of radial intercalation in the DMZ. Radial intercalation initially occurs in the animal region of the BCR, as epiboly extends the BCR to encompass the embryo during gastrulation. The early stages of epiboly occur before gastrulation initiates and are, therefore, independent of FN matrix assembly. A later phase of radial intercalation begins in the marginal zone at gastrulation (Keller, 1978) and contributes to the lengthening of the dorsal axis (Wilson and Keller, 1991). This later stage of epiboly in the marginal zone is coincident with the initiation of FN matrix assembly and is a prelude to convergent extension movements in the same tissue (Wilson and Keller, 1991). In embryos without a FN matrix, there is no evidence for spreading of the superficial layers, or radial intercalation in the deep layers of the DMZ, suggesting that there is a failure in epiboly and perhaps a subsequent failure of convergent extension.

The situation in the animal pole of the BCR is apparently different because the roof thins before the assembly of a FN matrix. In mAb-injected embryos, the roof thins and then undergoes a subsequent thickening after stage 10.5. Although the layer index of the BCR increases, this thickening is not due to increased proliferation of deep cells, because no increase in the number of mitotic indices in this cell population was observed in the absence of a FN matrix (data not shown). The randomization of spindle orientation in the absence of FN suggests that the increase in the BCR layer index is due to a loss of normal BCR cell orientation. Thus, it would appear that in the marginal zone, FN supports intercalation, while in the animal pole of the BCR it acts to stabilize the existing architecture. There is precedent for such an interpretation because the epiboly observed during gastrulation is biphasic (Keller, 1978) and the behaviors of deep cells in the animal cap and marginal zone are not equivalent (Keller, 1980a).

Observations in *Pleurodeles* also support a model in which there is a mechanistic difference in the epibolic movements of the BCR and the marginal zone. In *Pleurodeles*, superficial ectoderm involution occurs to a greater extent than in *Xenopus* and is dependent upon epiboly in the animal cap early in gastrulation. Disruption of FN/integrin interactions in this amphibian results in a thickened convoluted BCR (Johnson et al., 1993). This is what one would expect if FN-independent epiboly were to occur in the BCR while involution was blocked in the marginal zone.

One of the more intriguing observations to arise from analyses of *Xenopus* embryos that lack a FN matrix is the apparent dissociation of morphogenetic movements within the three primary germ layers. It is unlikely that this is the direct 'mechanical' result of a loss of integrin-FN ligation, and suggests that interruption of integrin/FN binding affects intracellular pathways that can alter the activity of other morphogenetic machines during gastrulation. Bottle cells form the dorsal lip, yet involution of superficial ectoderm does not occur, despite involution and extension of the deeper mesoderm. Several mechanisms have been proposed to drive the dorsal extension of deep mesoderm and endoderm cells during gastrulation (Keller and Tibbetts, 1989; Winklbauer and Schurfeld, 1999). Dissociation of these coordinated cellular rearrangements could result in increased tension at the dorsal lip and cause the characteristic buckling we observed in embryos that lack a FN matrix (Figs 3, 6J). It is significant that in both mouse (George et al., 1993) and chick (Harrisson et al., 1993), the absence of integrin/FN interactions in these embryos is associated with a shortened axis, ectodermal thickening and multiple mesodermal defects, some of the same characteristics that we observe in *Xenopus*. This suggests that integrin/FN ligation provides a signal that is essential in gastrulation and highly conserved across species.

FN is permissive for radial intercalation

Our evidence suggests that FN is required for BCR deep cell radial intercalation. Similar to what is observed in vivo, cells in the deep layer explant on a FN substrate undergo intercalation, while those on a non-adherent (BSA) substrate do not. There are several possible explanations to account for cell dependence on FN for intercalation. The simplest is that the FN substrate acts as a boundary and that as cells approach that boundary, they are captured. In our explant assay, many cells were observed to undergo intercalation distant from the substrate, suggesting that boundary capture is not the mechanism driving intercalation in this explant. A second possibility is that our results reflect simple mixing. This would suggest that adherence to FN signals a subsequent reduction in cell adhesion to FN (e.g. decreased integrin affinity and/or avidity) and increased adhesion to neighboring cells to promote cell mixing. This is again unlikely because in our assay, labeled cells initially adherent to FN are never observed to leave the substrate but more superficial cells can intercalate between them. In addition, cells distant from the FN substrate undergo intercalation activity without having contacted FN. This observation would suggest that the positional relationships between cells are altered upon integrin/FN ligation in the absence of any change in the ability of a cell to bind FN, and that this behavior is passed on to neighboring cells.

An interesting observation in these experiments is that FN is not required for patches of BCR deep cells to re-incorporate into the BCR (Fig. 8B-H). It is thought that the ability of BCR patches to re-incorporate is mediated through cadherins (Wacker et al., 2000). Our data suggest that FN can alter the way cells of the BCR interact with each other, possibly through 'crosstalk' with cadherins. It is unlikely that integrin binding to FN abolishes cadherin function, because the BCR remains intact. However, if integrin ligation modulated cadherin function and reduced cell-cell adhesion, this could promote cell rearrangements in the BCR without blocking incorporation (Zhong et al., 1999). We are presently examining the possibility that integrin ligation modulates cadherin function in the BCR during gastrulation.

Radial intercalation requires β1-containing integrins

Our use of antibodies that block the α5β1 integrin-binding sites on FN demonstrates that the cell behaviors we observe are integrin mediated. If FN conveys a signal via integrins across the plasma membrane, then it should be able to interfere with the intracellular transmission of this signal. The HAβ1 construct presumably acts as a dominant negative receptor by clustering β1 tails and depleting cytoplasmic components needed for the normal activity of endogenous β1-containing integrins, as reported previously for similar integrin chimeric constructs (Chen et al., 1994; LaFlamme et al., 1994). In embryos, these constructs give the same phenotypes with respect to BCR morphology as the mAb-dependent blocking of FN fibril assembly. This evidence supports the hypothesis that the effects we see are based upon integrin-mediated signals and that these signals are at least partially responsible for local radial intercalation behaviors in the DMZ.

FN matrix and cell polarity

In FN matrix-deficient embryos, the BCR thickens in the animal pole region and does not thin in the marginal zones during gastrulation. If thinning is driven through radial intercalation of multiple layers of BCR deep cells, then these cells must somehow interpret the vertical plane of the epithelium. Cell polarity is evident in the BCR in the uniform orientation of mitotic spindles within the horizontal plane of the epithelium in both the superficial and deep cell layers. One could imagine that tension across the BCR could influence spindle orientation. However, in embryos lacking a matrix, spindle orientation remains unchanged in the superficial layer, while it is randomized in deep layers. It is unlikely, therefore, that tension alone could account for spindle orientation in the BCR. Such an interpretation is further supported by the observation that small patches of dominant negative HAβ1 integrin expression disrupt morphogenesis locally (data not shown). Another possibility is that these deep cells have intrinsic polarity and that this directs mitotic spindle orientation in a manner similar to that reported for *Drosophila* (Eaton et al., 1995; Gho and Schweisguth, 1998).

Recent studies in *Xenopus* indicate that a pathway acting through Dishevelled, similar to the *Drosophila* planar cell polarity (PCP) cascade (Adler, 1992), may regulate cell polarity in the DMZ (Axelrod et al., 1998; Djiane et al., 2000; Rothbacher et al., 2000; Tada and Smith, 2000; Wallingford et al., 2000). Our results indicate that integrin ligation to FN can initiate the rapid relocalization of Dsh to the cell membrane. This occurs in stage 10 marginal zone tissue that undergoes

convergent extension, as well as in animal caps that do not. Because we do not manipulate either Wnt or Fz expression in these experiments, these results suggest that the deep cells of the BCR have the information needed to initiate Dsh relocalization but that FN can trigger the pathway prematurely. These effects are also specific to integrins, because we can block Dsh relocalization with an antibody (mAb 4B12; Ramos et al., 1996) that interferes with integrin binding to the CCBD of FN. Furthermore, Dsh localization to the plasma membrane is not supported by the non-integrin-dependent adhesive substrates poly-L-lysine and the HepII domain of FN. The Dsh mobilization that we report is not as robust as that seen when members of the Wnt signaling pathway are overexpressed (Boutros et al., 2000; Medina et al., 2000; Medina and Steinbeisser, 2000; Rothbacher et al., 2000; Umbhauer et al., 2000), but is comparable with that observed previously in the absence of overexpression of Wnts and/or their receptors (Wallingford et al., 2000). Although it has been proposed that membrane localization of Dsh may be an indication of a non-canonical Wnt signaling pathway (Axelrod et al., 1998; Wallingford et al., 2000), the physiological consequences of Dsh membrane localization remain unclear (Boutros et al., 2000; Medina et al., 2000; Umbhauer et al., 2000). Our experiments indicate that integrin/FN ligation is permissive for the initiation of polarity and is required for cell intercalation, and that this is correlated with the intracellular mobilization of Dsh to the cell membrane.

A role for FN induced polarity in the DMZ

In *Xenopus* embryos, cells of the DMZ undergo radial intercalation prior to mediolateral cell intercalation (Wilson and Keller, 1991), and can transmit the ability to intercalate to non-involuted tissue through physical contact (Keller et al., 1992b). We provide evidence that FN acting through integrins can confer polarized behavior to deep cells of the DMZ. Cell polarity is transmitted through cell-cell contact to cells distant from the substrate and is required for cells to undergo radial intercalation. It is likely that FN provides an integrin-dependent signal that allows for polarity to be established in the marginal zone. Interestingly, this putative signaling event permits the mobilization of Dsh, a molecule more frequently associated with the Wnt/Fz signaling pathways (Boutros and Mlodzik, 1999). Previous reports, however, have suggested a link between integrins and Wnt signaling (D'Amico et al., 2000; Novak et al., 1998; Tu et al., 1999; Yoganathan et al., 2000), as well as the mobilization of Dsh following integrin ligation (Torres and Nelson, 2000). Significantly, interference with XFz7 (Djiane et al., 2000), XWnt11 (Tada and Smith, 2000) or Dsh (Wallingford et al., 2000) in the DMZ blocks convergent extension movements and alters cell-cell adhesion (Medina et al., 2000) without altering the ability of cells to adhere to FN (M. M., G. N. Wheeler and D. W. D., unpublished; Tada and Smith, 2000). Our model predicts that integrin signaling is in a pathway parallel to that described for Wnt/Fz, and that interplay between these pathways, possibly through Dsh, establishes cell polarity in the DMZ of the embryo within a correct temporal framework. While the molecules that mediate cell polarity continue to be characterized, the signals that provide the initial asymmetry required for the development of polarity remain unknown. Our evidence suggests that FN matrix may provide a cue important in the establishment of cellular asymmetry that is crucial to subsequent morphogenetic rearrangements in *Xenopus*.

The authors thank Randy Moon, Jeffery Miller, Ray Keller, Paul Adler, Dominique Alfandari and Sergei Sokol for discussions useful in the preparation of this manuscript. We also thank David Ransom for preparing the HAβ1 construct and Sandra Kateeshock for initial characterization of the phenotype. This work was supported by grants from the USPHS (HD26402 and HD01104) and the American Cancer Society (RPG93-038-06-CSM).

REFERENCES

Adler, P. N. (1992). The genetic control of tissue polarity in Drosophila. *BioEssays* **14**, 735-741.

Axelrod, J. D., Miller, J. R., Shulman, J. M., Moon, R. T. and Perrimon, N. (1998). Differential recruitment of Dishevelled provides signaling specificity in the planar cell polarity and Wingless signaling pathways. *Genes Dev.* **12**, 2610-2622.

Boucaut, J. C. and Darribere, T. (1983a). Fibronectin in early amphibian embryos. Migrating mesodermal cells contact fibronectin established prior to gastrulation. *Cell Tissue Res.* **234**, 135-145.

Boucaut, J. C. and Darribere, T. (1983b). Presence of fibronectin during early embryogenesis in amphibian Pleurodeles waltlii. *Cell Differ.* **12**, 77-83.

Boutros, M. and Mlodzik, M. (1999). Dishevelled: at the crossroads of divergent intracellular signaling pathways. *Mech. Dev.* **83**, 27-37.

Boutros, M., Mihaly, J., Bouwmeester, T. and Mlodzik, M. (2000). Signaling specificity by Frizzled receptors in Drosophila. *Science* **288**, 1825-1828.

Chen, Y. P., O'Toole, T. E., Shipley, T., Forsyth, J., LaFlamme, S. E., Yamada, K. M., Shattil, S. J. and Ginsberg, M. H. (1994). 'Inside-out' signal transduction inhibited by isolated integrin cytoplasmic domains. *J. Biol. Chem.* **269**, 18307-18310.

Collazo, A., Fraser, S. E. and Mabee, P. M. (1994). A dual embryonic origin for vertebrate mechanoreceptors. *Science* **264**, 426-430.

Cooke, J. and Smith, E. J. (1988). The restrictive effect of early exposure to lithium upon body pattern in Xenopus development, studied by quantitative anatomy and immunofluorescence. *Development* **102**, 85-99.

D'Amico, M., Hulit, J., Amanatullah, D. F., Zafonte, B. T., Albanese, C., Bouzahzah, B., Fu, M., Augenlicht, L. H., Donehower, L. A., Takemaru, K. I. et al. (2000). The integrin-linked kinase regulates the cyclin D1 gene through glycogen synthase kinase 3beta and cAMP-responsive element-binding protein-dependent pathways. *J. Biol. Chem.* **275**, 32649-32657.

Darribere, T. and Schwarzbauer, J. E. (2000). Fibronectin matrix composition and organization can regulate cell migration during amphibian development. *Mech. Dev.* **92**, 239-250.

Darribere, T., Yamada, K. M., Johnson, K. E. and Boucaut, J. C. (1988). The 140-kDa fibronectin receptor complex is required for mesodermal cell adhesion during gastrulation in the amphibian Pleurodeles waltlii. *Dev. Biol.* **126**, 182-194.

Darribere, T., Guida, K., Larjava, H., Johnson, K. E., Yamada, K. M., Thiery, J. P. and Boucaut, J. C. (1990). In vivo analyses of integrin beta 1 subunit function in fibronectin matrix assembly. *J. Cell Biol.* **110**, 1813-1823.

Darribere, T., Koteliansky, V. E., Chernousov, M. A., Akiyama, S. K., Yamada, K. M., Thiery, J. P. and Boucaut, J. C. (1992). Distinct regions of human fibronectin are essential for fibril assembly in an in vivo developing system. *Dev. Dyn.* **194**, 63-70.

Davidson, L. A. and Keller, R. E. (1999). Neural tube closure in Xenopus laevis involves medial migration, directed protrusive activity, cell intercalation and convergent extension. *Development* **126**, 4547-4556.

DeSimone, D. W. (1994). Adhesion and matrix in vertebrate development. *Curr. Opin. Cell Biol.* **6**, 747-751.

Djiane, A., Riou, J., Umbhauer, M., Boucaut, J. and Shi, D. (2000). Role of frizzled 7 in the regulation of convergent extension movements during gastrulation in xenopus laevis. *Development* **127**, 3091-3100.

Doms, R. W., Gething, M. J., Henneberry, J., White, J. and Helenius, A. (1986). Variant influenza virus hemaglutinin that induces fusion at elevated pH. *J. Virol.* **57**, 603-613.

Eaton, S., Auvinen, P., Luo, L., Jan, Y. N. and Simons, K. (1995). CDC42

and Rac1 control different actin-dependent processes in the Drosophila wing disc epithelium. *J. Cell Biol.* **131**, 151-164.

Gard, D. L. (1993). Confocal immunofluorescence microscopy of microtubules in amphibian oocytes and eggs. *Methods Cell Biol.* **38**, 241-264.

Gawantka, V., Joos, T. O. and Hausen, P. (1994). A beta 1-integrin associated alpha-chain is differentially expressed during Xenopus embryogenesis. *Mech. Dev.* **47**, 199-211.

George, E. L., Georges-Labouesse, E. N., Patel-King, R. S., Rayburn, H. and Hynes, R. O. (1993). Defects in mesoderm, neural tube and vascular development in mouse embryos lacking fibronectin. *Development* **119**, 1079-1091.

Gho, M. and Schweisguth, F. (1998). Frizzled signalling controls orientation of asymmetric sense organ precursor cell divisions in Drosophila. *Nature* **393**, 178-181.

Harrisson, F., Van Nassauw, L., Van Hoof, J. and Foidart, J. M. (1993). Microinjection of antifibronectin antibodies in the chicken blastoderm: inhibition of mesoblast cell migration but not of cell ingression at the primitive streak. *Anat. Rec.* **236**, 685-696.

Heisenberg, C. P., Tada, M., Rauch, G. J., Saude, L., Concha, M. L., Geisler, R., Stemple, D. L., Smith, J. C. and Wilson, S. W. (2000). Silberblick/Wnt11 mediates convergent extension movements during zebrafish gastrulation. *Nature* **405**, 76-81.

Howard, J. E., Hirst, E. M. and Smith, J. C. (1992). Are beta 1 integrins involved in Xenopus gastrulation? *Mech. Dev.* **38**, 109-119.

Hynes, R. O. (1990). *Fibronectins*. New York: Springer-Verlag.

Johnson, K. E., Darribere, T. and Boucaut, J. C. (1993). Mesodermal cell adhesion to fibronectin-rich fibrillar extracellular matrix is required for normal Rana pipiens gastrulation. *J. Exp. Zool.* **265**, 40-53.

Kao, K. R. and Elinson, R. P. (1988). The entire mesodermal mantle behaves as Spemann's organizer in dorsoanterior enhanced Xenopus laevis embryos. *Dev. Biol.* **127**, 64-77.

Keller, R. and Tibbetts, P. (1989). Mediolateral cell intercalation in the dorsal, axial mesoderm of Xenopus laevis. *Dev. Biol.* **131**, 539-549.

Keller, R. and Jansa, S. (1992). Xenopus gastrulation without a blastocoel roof. *Dev. Dyn.* **195**, 162-176.

Keller, R. and Winklbauer, R. (1992). Cellular basis of amphibian gastrulation. *Curr. Top. Dev. Biol.* **27**, 39-89.

Keller, R., Shih, J. and Domingo, C. (1992a). The patterning and functioning of protrusive activity during convergence and extension of the Xenopus organiser. *Development* **114**, 81-91.

Keller, R., Shih, J., Sater, A. K. and Moreno, C. (1992b). Planar induction of convergence and extension of the neural plate by the organizer of Xenopus. *Dev. Dyn.* **193**, 218-234.

Keller, R. E. (1978). Time-lapse cinemicrographic analysis of superficial cell behavior during and prior to gastruation in *Xenopus laevis*. *J. Morphol.* **157**, 223-248.

Keller, R. E. (1980a). The cellular basis of epiboly: an SEM study of deep-cell rearrangement during gastrulation in Xenopus laevis. *J. Embryol. Exp. Morphol.* **60**, 201-234.

Keller, R. E. (1980b). The cellular basis of epiboly: an SEM study of deep-cell rearrangement during gastrulation in *Xenopus laevis*. *J. Embryol. Exp. Morphol.* **60**, 201-234.

Klein, S. L. and Moody, S. A. (1989). Lithium changes the ectodermal fate of individual frog blastomeres because it causes ectopic neural plate formation. *Development* **106**, 599-610.

LaFlamme, S. E., Thomas, L. A., Yamada, S. S. and Yamada, K. M. (1994). Single subunit chimeric integrins as mimics and inhibitors of endogenous integrin functions in receptor localization, cell spreading and migration, and matrix assembly. **126**, 1287-1298.

Lee, G., Hynes, R. and Kirschner, M. (1984). Temporal and spatial regulation of fibronectin in early Xenopus development. *Cell* **36**, 729-740.

Medina, A. and Steinbeisser, H. (2000). Interaction of Frizzled 7 and Dishevelled in Xenopus. *Dev. Dyn.* **218**, 671-680.

Medina, A., Reintsch, W. and Steinbeisser, H. (2000). Xenopus frizzled 7 can act in canonical and non-canonical Wnt signaling pathways: implications on early patterning and morphogenesis. *Mech. Dev.* **92**, 227-237.

Nakatsuji, N. (1986). Presumptive mesoderm cells from Xenopus laevis gastrulae attach to and migrate on substrata coated with fibronectin or laminin. *J. Cell Sci.* **86**, 109-118.

Nakatsuji, N. and Johnson, K. E. (1983). Conditioning of a culture substratum by the ectodermal layer promotes attachment and oriented locomotion by amphibian gastrula mesodermal cells. *J. Cell Sci.* **59**, 43-60.

Nakatsuji, N., Smolira, M. A. and Wylie, C. C. (1985). Fibronectin visualized by scanning electron microscopy immunocytochemistry on the substratum for cell migration in Xenopus laevis gastrulae. *Dev. Biol.* **107**, 264-268.

Novak, A., Hsu, S. C., Leung-Hagesteijn, C., Radeva, G., Papkoff, J., Montesano, R., Roskelley, C., Grosschedl, R. and Dedhar, S. (1998). Cell adhesion and the integrin-linked kinase regulate the LEF-1 and beta-catenin signaling pathways. *Proc. Natl. Acad. Sci. USA* **95**, 4374-4379.

Ojakian, G. K. and Schwimmer, R. (1994). Regulation of epithelial cell surface polarity reversal by beta 1 integrins. *J. Cell Sci.* **107**, 561-576.

Ramos, J. W. and DeSimone, D. W. (1996). Xenopus embryonic cell adhesion to fibronectin: position-specific activation of RGD/synergy site-dependent migratory behavior at gastrulation. *J. Cell Biol.* **134**, 227-240.

Ramos, J. W., Whittaker, C. A. and DeSimone, D. W. (1996). Integrin-dependent adhesive activity is spatially controlled by inductive signals at gastrulation. *Development* **122**, 2873-2883.

Regen, C. and Steinhardt, R. (1988). Lithium dorsalizes but also mechanically disrupts gastrulation of *Xenopus laevis*. *Development* **102**, 677-686.

Riou, J. F., Shi, D. L., Chiquet, M. and Boucaut, J. C. (1990). Exogenous tenascin inhibits mesodermal cell migration during amphibian gastrulation. *Dev. Biol.* **137**, 305-317.

Rothbacher, U., Laurent, M. N., Deardorff, M. A., Klein, P. S., Cho, K. W. and Fraser, S. E. (2000). Dishevelled phosphorylation, subcellular localization and multimerization regulate its role in early embryogenesis. *EMBO J.* **19**, 1010-1022.

Sechler, J. L., Corbett, S. A. and Schwarzbauer, J. E. (1997). Modulatory roles for integrin activation and the synergy site of Fibronectin during Matrix Assembly. *Mol Biol Cell* **8**, 2563-2573.

Tada, M. and Smith, J. C. (2000). Xwnt11 is a target of Xenopus Brachyury: regulation of gastrulation movements via Dishevelled, but not through the canonical Wnt pathway. *Development* **127**, 2227-2238.

Torres, M. A. and Nelson, W. J. (2000). Colocalization and redistribution of dishevelled and actin during Wnt- induced mesenchymal morphogenesis. *J. Cell Biol.* **149**, 1433-1442.

Tu, Y., Li, F., Goicoechea, S. and Wu, C. (1999). The LIM-only protein PINCH directly interacts with integrin-linked kinase and is recruited to integrin-rich sites in spreading cells. *Mol. Cell. Biol.* **19**, 2425-2434.

Umbhauer, M., Djiane, A., Goisset, C., Penzo-Mendez, A., Riou, J. F., Boucaut, J. C. and Shi, D. L. (2000). The C-terminal cytoplasmic lys-thr-X-X-X-Trp motif in frizzled receptors mediates Wnt/beta-catenin signalling. *EMBO J.* **19**, 4944-4954.

Wacker, S., Grimm, K., Joos, T. and Winklbauer, R. (2000). Development and control of tissue separation at gastrulation in Xenopus. *Dev. Biol.* **224**, 428-439.

Wallingford, J. B., Rowning, B. A., Vogeli, K. M., Rothbacher, U., Fraser, S. E. and Harland, R. M. (2000). Dishevelled controls cell polarity during Xenopus gastrulation. *Nature* **405**, 81-85.

Watt, F. M., Kubler, M. D., Hotchin, N. A., Nicholson, L. J. and Adams, J. C. (1993). Regulation of keratinocyte terminal differentiation by integrin-extracellular matrix interactions. *J. Cell Sci.* **106**, 175-182.

Wilson, P. and Keller, R. (1991). Cell rearrangement during gastrulation of Xenopus: direct observation of cultured explants. *Development* **112**, 289-300.

Winklbauer, R. (1989). Development of the lateral line system in Xenopus. *Prog. Neurobiol.* **32**, 181-206.

Winklbauer, R. (1990). Mesodermal cell migration during Xenopus gastrulation. *Dev. Biol.* **142**, 155-168.

Winklbauer, R. and Keller, R. E. (1996). Fibronectin, mesoderm migration, and gastrulation in Xenopus. *Dev. Biol.* **177**, 413-426.

Winklbauer, R. and Schurfeld, M. (1999). Vegetal rotation, a new gastrulation movement involved in the internalization of the mesoderm and endoderm in Xenopus. *Development* **126**, 3703-3713.

Winklbauer, R. and Stoltz, C. (1995). Fibronectin fibril growth in the extracellular matrix of the Xenopus embryo. *J. Cell Sci.* **108**, 1575-1586.

Yeaman, C., Grindstaff, K. K. and Nelson, W. J. (1999). New perspectives on mechanisms involved in generating epithelial cell polarity. *Physiol. Rev.* **79**, 73-98.

Yoganathan, T. N., Costello, P., Chen, X., Jabali, M., Yan, J., Leung, D., Zhang, Z., Yee, A., Dedhar, S. and Sanghera, J. (2000). Integrin-linked kinase (ILK): a 'hot' therapeutic target. *Biochem. Pharmacol.* **60**, 1115-1119.

Zhong, Y., Brieher, W. M. and Gumbiner, B. M. (1999). Analysis of C-cadherin regulation during tissue morphogenesis with an activating antibody. *J. Cell Biol.* **144**, 351-359.